Mansoura University
Faculty of Engineering
Mansoura Engineering Journal

Performance Evaluation of Asphalt Mixtures Modified with Nanomaterials

Talaat Abdel-Wahed, Ashraf Abdel-Raheem and Ghada S. Moussa

KEYWORDS:
modified asphalt mixture; Nano-Clay, Nano-Silica, Creep, double-punch, FTIR, moisture sensitivity

***Abstract*—Recently, nanomaterials have been widely used to improve the properties of asphalt binders due to their unique properties. This research aims to evaluate the performance of nano-modified binders with two different types of nanomaterials, which are Nano-Silica (NS) and Nano-Clay (NC). Each of them was added to a 60/70 penetration grade bitumen at concentrations ranging from 1% to 4% by asphalt binder weight using a high shear mixer at a speed of 4000 rpm and a mixing temperature of 145 °C for 60 minutes. A number of basic tests were carried out on the binders, such as penetration grade, softening point, rotational viscosity, and stability storage tests. Moreover, Scanning Electron Microscope (SEM) and Fourier Transform Infrared (FTIR) tests were utilized to ensure the quality of the mixing process and investigate the modified binder's internal composition. Furthermore, an additional laboratory study was carried out to characterize the performance properties of the corresponding asphalt concrete (AC) mixtures based on the Marshall stability, indirect tensile strength, moisture susceptibility, double-punch, and static creep tests. Based on the experimental results, the best performance was attained when incorporating 3-4% nanoparticles with a neat asphalt binder. In general, the addition of NS or NC particles positively affected the asphalt binder and AC mixture in terms of stability, debonding, moisture damage, and rutting. However, NC was more effective compared to NS and can be used to build sturdy pavements**

I. INTRODUCTION

TRADITIONAL asphalt needs further improvements due to many problems, such as moisture susceptibility, debonding, and permanent deformation [1–3]. Recently, the use of nanomaterials to improve the performance of asphalt binder and hot mix asphalt (HMA) has become more widespread. Several kinds of nanoparticles have been used to modify HMA mixes, such as Nano-Carbon tubes, Nano-Clay (NC), Nano-Silica (NS), Nano-Polymers (NP), etc. Furthermore, authors in [4,5] studied the impact of incorporating NC particles into HMA on the performance of high-density polyethylene (HDPE)-modified AC mixture. Recently, among many other additives, nanoparticles have shown encouraging potential in enhancing the performance of AC mixtures.

Nanomaterials exhibit specific properties such as large surface area, small size, high dispersion ability, good absorption, high stability, and chemical purity compared to common additives, making them an effective additive to improve AC mixtures [6–9]. Previous studies have shown that

Received: (08 November, 2021) - Revised: (09 January, 2022) - Accepted: (10 January, 2022)

***Corresponding Author:** Talaat Abdel-Wahed is an Associate Professor at the Civil Engineering Department, Faculty of Engineering at Sohag University, Sohag, Egypt (e-mail: dr.talaat_ali@eng.sohag.edu.eg)*

Ashraf Abdel-Raheem is an Assistant Lecturer at the Civil Engineering Department, Faculty of Engineering at Sohag University, Sohag, Egypt (e-mail: ashrf_salah@eng.sohag.edu.eg)

Ghada S. Moussa is a Professor of Highway and Traffic Engineering, Civil Engineering Department, Faculty of Engineering, Assiut University, Assiut, Egypt, on leave to Sphinx University, Egypt (e-mail: ghada.moussa@aun.edu.eg)

(Ser. NO. BFEMU-2110-1182)

nanomaterials positively affect AC mixtures by improving the cohesion and adhesion between aggregate and binder [10,11]. The nanomaterials improve the asphalt binder's stiffness, which increases the mixture's resistance to rutting [10,12–14]

Previous studies modified asphalt binder (60/70) by adding 2%, 4%, and 6% of NS using a high shear mixer at speeds ranging from 1800 rpm to 6000 rpm and a mixing temperature ranging from 140 ºC to 180 ºC for a period not less than 30 minutes [15–19]. Their results revealed an improvement in the properties of the asphalt binder and that the binder became less sensitive to temperature [15,17,18]. Taherkhani et al. [15] reported a slight improvement in the moisture resistance of the AC mixture when they used NS to modify it. Similar results regarding moisture sensitivity were attained when Kavussi et al. [20] added NC with the same proportions of NS to asphalt binder (PG 58-22). Ezzat et al. [21] investigated the effect of adding NS and NC on the properties of the asphalt binder. The nanomaterials were used individually at rates ranging from 1% to 7%, utilizing a high shear mixer (1500 rpm). Their study exhibited a decrease in penetration depth with an increase in the softening point temperature and the rotational viscosity. It was also noticed that NC is more effective than NS for improving the physical properties of asphalt binders.

Furthermore, NS with a content of 1%, 3%, and 5% by weight of binder was utilized [1,12,22]. They reported an increase in the asphalt binder's hardness with decreased thermal sensitivity. Also, an improvement in rutting resistance and Marshall stability values were attained. Sadeghnejad et al. [23] evaluated the effect of adding NS and Nano-TiO2 on the behavior of stone mastic AC mixtures. The main outcomes of their study showed that Nano-TiO2 was more effective in reducing moisture sensitivity and improving fatigue and rutting parameters than NS. Other investigations introduced Nano-TiO2 as an additive to asphalt binder. They concluded that adding Nano TiO2 to the asphalt binder improved the asphalt binder’s basic properties its resistance to rutting [11,24–26]. Two studies used NS with low contents: Saltan et al. [27] and Sadeghnejad et al. [25]. Saltan et al. added NS to asphalt binder at concentrations from 0.1% to 0.5% NS and recorded an increase in rotational viscosity and the indirect tensile ratio (TSR). However, Sadeghnejad et al. tested NS with dosages of 0.1%-1.2% NS using a shear mixer at a speed of 4000 rpm. The results showed an improvement in the asphalt binder’s performance, especially its resistance to permanent deformations. Al-Taher et al. [28] found that NS at contents from 3% to 11% increases Marshall stability and indirect tensile stress. The wheel track test also revealed a decrease in the tendency of the AC mixtures to deform. Similar performance to this study regarding Marshall stability and indirect tensile stress was obtained by Zakaria et al. [29] when NC was added in contents ranging from 2% to 8%. Hamedi et al. [30] reported that inserting Nano-Zinc into an asphalt binder enhances its resistance to moisture damage. Saltan et al. [31] modified a binder (PG 64-22) utilizing a Multi-Walled Carbon Nanotube (MWCNT). An improvement in the properties of the nano-modified binder and AC mixture was observed, represented by increased Marshall stability, and decreased sensitivity to moisture. Finally, Kavussi et al. [20] suggested adding 5% Nano Hydrated Lime (NHL) to asphalt binder (PG 58-22) to obtain the best performance in terms of moisture sensitivity. Recent contributions in nanoparticles-based asphalt modifiers are summarized in Table 1.

Although several studies have been conducted on using nanomaterials in AC mixtures, the performance of asphalt binders and AC mixes using NS and NC has not been fully addressed. Wherein, more investigations are needed to understand their applicability and the direct influence of both nanoparticles on the binder behavior as well as the mixture behavior. Thus, this research aims to assess the performance of asphalt binders and HMA mixes modified with NC and NS. Furthermore, their physical properties, storage stability, and chemical change were examined. Besides, the HMA mixtures’ stiffness, moisture damage susceptibility, debonding, and rutting tendency, are assessed. To accomplish this, numerous binders and HMA mixes tests are performed. The penetration grade, ring and ball, rotational viscosity tests are conducted to study binder's physical characteristics and storage stability. Modified asphalt binders' chemical characteristics and structural patterns are investigated via Fourier Transform Infrared (FTIR) and Scanning Electron Microscopy (SEM) tests. Moreover, various tests for HMA mixtures’ assessment were considered (i.e., Marshall, Immersion–compression, Double punching, static creep tests for stiffness, moisture damage susceptibility, deponding, and rutting resistance, respectively).

II. EXPERIMENTAL PROGRAM

2.1 Materials

Aggregate and asphalt binder are the main components of AC mixtures. This section describes the main characteristics of the selected aggregate and asphalt additives (NC and NS) that were used in this research. The following subsections present the characteristics of these investigated materials.

2.1. 1 Asphalt binder

Virgin 60/70 penetration grade bitumen from the Suez refinery has been chosen as the base binder. The physical properties of the asphalt binder are given in Table 2.

2.1.2 Aggregate

Crushed dolomite stones with a rough surface texture were used as a coarse aggregate. Natural sand was selected as a fine aggregate. Various proportions of aggregate were tried until the final aggregate gradation was within gradation limits of a wearing surface (4C) course according to the Egyptian specifications [29]. Fig 1 shows the final selected gradation of aggregates along with the specification limits. Table 3 displays the physical properties of aggregates.

2.1.3 Additives

Two types of nanoparticles were investigated in this research, namely NC and NS, and they are pictured in. Fig 2. their physical and chemical properties are shown in Table 4.

TABLE I
SUMMARY OF LITERATURE STUDIES ON NANOPARTICLES AS MODIFIERS TO ASPHALT BINDERS AND/OR MIXES *

Nanomaterial content (%)	Binder Type	Mixing Condition			Binder/Mixture Performance													Ref.
		Speed (rpm)	Temp. (ºC)	Duration (min.)	P	S	V	D	ST	MS	ITS	SM	TSR	Mr	R	F	TS	
4% Nano TiO_2	60/70	700		45	↘	↗	↗	↗							↗			[11]
(1%, 3%, 5%, and 7%) Nano TiO_2	60/70				↘	↗	↑	↑							↗	↗	↘	[24]
(2%, 4%, 6%) NS	60/70	4000	180	120	↘	↗		↘							↑			[19]
(5%, 10%, 20%) NHL	PG 58-22	3500	160	40							↗		↗					[20]
(2%, 4%, 6%) NC	PG 58-22	5200	155	30							↗		↗					[20]
(1%, 2%, 3%,4%,5%,6%,7%) NS	56 dmm	1500	145 ± 5	60	↘	↗	↗											[21]
(1%, 2%, 3%,4%,5%,6%,7%) NC	56 dmm	1500	145 ± 5	60	↘	↗	↗											[21]
(1%, 3%, 5%) NS	60/70	3000	160	60	↘	↗		↘									↘	[12]
(2%, 4%) Nano- ZnO	60/70	14000	130–140	4-5							↗		↗					[30]
(0.3, 0.6, 0.9 and 1.2%) NS	60/70	4000	150								↗	↗	↗		↗	↗		[23]
(0.3, 0.6, 0.9 and 1.2%) Nano TiO_2	60/70	4000	150								↗	↗	↗		↗	↗		[23]
(0.1%, 0.3%, 0.5%) NS	PG64-22	4000	160	120			↘				↗		↗		↘			[27]
(3, 5, 7,9, 11%) NS	60/70		150		↘	↗				↗	↗				↘			[28]
(2%, 4%, 6%, 8%) NC	60/70	600	120-130	30	↘	↗	↗			↗	↗							[29]
(0.3, 0.6, 0.9 and 1.2%) NS	60/70	4000	150		↘	↗	↗								↗			[25]
(0.3, 0.6, 0.9 and 1.2%) Nano TiO_2	60/70	4000	150		↘	↗	↗								↗			[25]
(2%, 4%, 6%) Nano TiO_2	77 dmm	5000-8000	130-150	30-40	↘	↗	↗									↘		[26]
(1%, 3%, 5%) NS	60/70	3000	160	60	↘	↗		↘		↗	↗		↗	↗	↗	↗	↘	[1]
(1%, 3%, 5%) NS	60/70	3000	160	60						↗					↗			[22]
(1%, 3%, 5%) MWCNT	PG 64-22	4000	160	120	↘	↗	↗	↘			↗		↗		↗			[31]
(2%, 4%, 6%) NS	60/70	4000	160	40	↘	↗		↘			↗		↗	↗		↗	↘	[15]
(2%, 4%, 6%) NS	60/70	2000-6000	140	30-60	↘	↗	↗	↘									↘	[17]
(2%, 4%, 6%) NS	60/70	2000	160	30-60	↘	↗	↗	↘									↘	[18]

* P = penetration; S = softening point; V = viscosity; D = ductility; ST= storage stability; MS = Marshall stability; ITS = Indirect tensile strength; TSR= tensile strength ratio; R = rutting parameter; SM = stiffness modulus; F= fatigue parameters; Mr = resilient mod-ulus; TS= temperature sensitivity. ↑ = Significant Increase; ↗ = Slight Increase; ↘ = Slight Decrease

TABLE II
PHYSICAL AND MECHANICAL CHARACTERISTICS OF THE ASPHALT BINDER

Test	Standard Test Method	Result
Penetration (at 25 °C, 5 sec.), 0.1mm	ASTM D5	62
Ductility (at 25 °C, 5 cm/min), cm	ASTM D113	+100
Softening Point (ring and ball), °C	ASTM D36	45.4
Kinematic viscosity (at 135 °C), C.st	ASTM D 2170	376
Flash point, °C	ASTM D92	+250
Density in 15 °C, g/cm3	ASTM-D70	1.01
Penetration index (PI)		-1.95

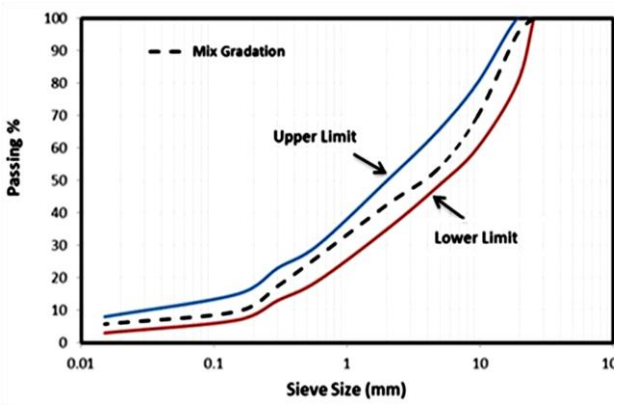

Fig. 1. Wearing surface layer (4C) specification limits and aggregates' blending gradation

TABLE III
PHYSICAL PROPERTIES OF AGGREGATES

Test	Results				Standard Test Method
	Agg. #1	Agg. #2	Sand	Filler	
Bulk Specific Gravity	2.583	2.576	2.514	---	ASTM C127 ASTM C128 ASTM D854
SSD Specific Gravity	2.624	2.622	2.531	---	
Apparent Specific Gravity	2.650	2.705	2.603	2.701	
Water Absorption (%)	1.95	2.04	2.89	---	
Disintegration in Water (%)	0.0	0.0	---	---	ASTM C88
Los Angeles	27.9	33.3	---	---	ASTM C131

The investigated nanomaterials were first characterized using X-ray diffraction (XRD). As shown in Fig 3, XRD spectrum of nanoparticles showed a strong diffraction peak at $2\theta = 27^\circ$ and $2\theta = 22^\circ$ with an interlay spacing (d) of 0.33 nm and 0.4 nm for NC and NS, respectively. The nanomaterials were also analyzed using Transmission Electronic Microscopy (TEM) to evaluate their practical size distribution in their dry powder state. However, the particles tend to cluster and form batches. Fig 4b shows a 30 to 50 nm particle size range for NS. It can be seen from the two figures that the investigated NC is much finer compared to NS, but neither of the nanoparticles exceeded the 100 nm limit used to decide if something is a nanomaterial according to ASTM E2456-06 [30].

2.2 Samples' Preparation

A high-shear mixer was utilized for mixing NC and NS with the base asphalt binder. NC and NS were used separately at concentrations ranging from 1% to 4% by weight of asphalt binder. The two nanomaterials were mixed with asphalt (60/70) at a temperature of 145 °C and a mixing speed of 4000 rpm for 60 minutes. Using the Marshall method (ASTM D 1559) [31], a conventional AC mixture was designed. It was found that the optimum asphalt content (OAC) was 5%. The same proportion of asphalt binder was used when preparing the nano-modified AC mixtures. Table 5 presents the characteristics of the conventional AC mixture and their limits according to the Egyptian specifications [29]. In both the binder and mixture tests, three samples were made from each concentration of nanoparticles, and the average values were taken.

(a) Nano-Clay Powder

(b) Nano-Silica Powder

Fig. 2. Nanoparticles used in study

TABLE IV
CHEMICAL AND PHYSICAL PROPERTIES OF NANOPARTICLES

[Property	Nano-Clay	Nano-Silica
Chemical formula	$Al_2Si_2O_5(OH)_4$	SiO_2
Purity (%)	>99%	99.5%
Specific gravity (g/cm^3)	2.6	1.08
Molecular weight (g/mole)	258.2	60.06
Melting Point (°C)	> 1500	1713
PH	4-6	3.7-4.5
Form	Powder	Powder
Colour	Cream	White

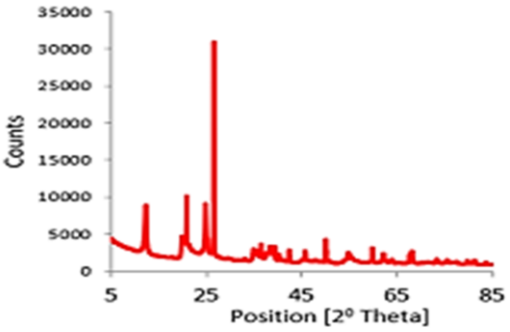

(b) Nano-Clay

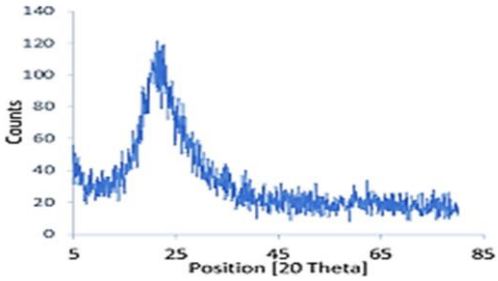

(b) Nano-Silica

Fig. 3. XRD patterns of Nano-Clay powder and Nano-Silica

TABLE V
MARSHALL DESIGN PARAMETERS FOR THE CONVENTIONAL AC MIXTURE

Marshall Parameter	Value	Specification*	
		Min.	Max.
bulk density, t/m³	2.35	-	-
Stability, kg	979.5	900	-
Flow, mm	3.83	2	4
Air voids (AV), %	4.32	3	5
Voids in mineral aggregates (VMA), %	15.83	13	-
Voids filled with binder (VFB), %	72.7	70	-
Optimum asphalt content (OAC), %	5	-	-
**According to the Egyptian Highway standard*			

2.3 Testing asphalt binder

To assess the hardness of the asphalt binder, a penetration grade test was carried out according to ASTM D5 [35]. Ring and ball test ASTM D36 [36] and rotational viscosity test ASTM D2171 [37] were used to measure the consistency and flow of the binder.

2.3.1 Temperature sensitivity

Depending on the penetration depth value and the softening point temperature, the penetration index (PI) was calculated according to Equation (1) [38]. This parameter indicates the temperature sensitivity of the binder, as the PI value is inversely proportional to its temperature sensitivity.

$$PI = \frac{1952 - 500\,log\,P_{25} - 20T_{R\&B}}{50 log P_{25} - T_{R\&B} - 120} \quad (1)$$

Where P25 and TR&B are the penetration value at 25 °C (in 0.1 mm increments) and softening point temperature (in °C), respectively.

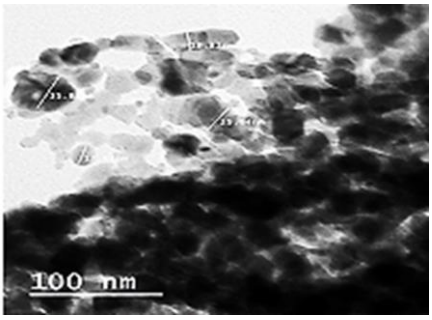

(a)Nano-Clay

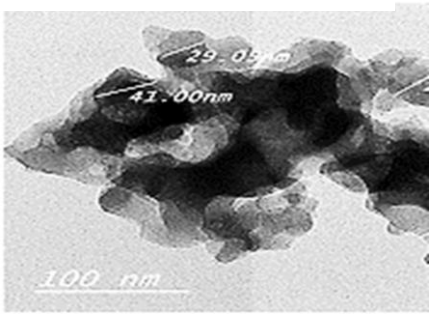

(b) Nano-Silica

Fig. 4. Nanoparticles under TEM

2.3.2 Storage stability

The storage stability test is used to check whether the modified binder is susceptible to separating the modifier and the binder at high temperatures [39,40]. According to ASTM D5892 [41], a liquid asphalt binder is poured into an aluminum tube. This tube is kept in an upright position at a temperature of 163 °C for 48 hours, and then kept in the refrigerator at a temperature of -7 °C for 4 hours. Finally, the tube is divided horizontally into three equal pieces, and a softening point test is performed for its upper and lower parts. The difference in softening point temperature is calculated between these upper and lower parts. If the difference is less than 2.2 °C, the asphalt binder is considered stable in storage.

2.3.3 Scanning electron microscopy (SEM)

To evaluate the dispersion of nanoparticles within asphalt binder, a Scanning Electron Microscopy (SEM) test was conducted on the base and nano-modified binder [42,43]. In this test, a sample with dimensions of (20 x 20 x 10) mm is used after coating it with a gold alloy to increase the hardness of its surface without affecting the surface's morphology [44]. SEM was operated at an acceleration voltage of 15 kev using a secondary electron (SE) signal.

2.3.4 Fourier transform infrared spectroscopy (FTIR)

An FTIR spectroscopy test was performed to detect the potential chemical interaction between neat binder and nanoparticles [7,45,46]. In this analysis, infrared radiation is passed through the asphalt sample; part of the radiation is absorbed while the other part is transmitted through the sample. The molecular fingerprint of the sample is obtained through the resulting signal on the detector in the form of a spectrum [47]. Using the correlation table, the functional groups are determined between the carbon and other groups of asphalt binder. In this study, the transmission FTIR spectra of the control and nano-modified binder were taken in the range 4500–500 cm-1.

2.4 Testing AC mixture

2.4.1 Marshall test

A Marshall test was performed to assess the tolerance to distortion, displacement, rutting, and shear stress of AC mixes [48]. The design process of the Marshall mix is usually carried out according to ASTM D 1559 [34]. Marshall hammer compacting (75 blows on each side) was used to produce cylindrical asphalt samples with a diameter of 101.6 mm and thickness 65–75 mm. Compacted samples were submerged in water at 60 °C for 30-40 minutes. Using the Marshall apparatus, samples were loaded at a rate of 50.8 mm/min until failure. During the loading process, the highest load is measured as the Marshall stability (Ms), and the vertical deformation at the highest load is measured using the dial gauge as the flow value (F). The AC mixture's resistance to permanent deformation can also be described in this test by calculating the Marshall quotient (MQ), which is defined as the ratio of Marshall stability (Kg) to flow (mm) [49].

2.4.2 Moisture susceptibility

Moisture susceptibility (moisture damage) is one of the most fundamental problems of asphalt pavements. Moisture susceptibility can be characterized as reducing the stiffness and durability of AC mixtures induced by moisture [43]. In this study, moisture resistance was investigated using two tests:

2.4.2.1 Indirect tensile strength (IDT)

An indirect tensile strength (IDT) test was carried out in compliance with AASHTO T 283 [50]. For each type of AC mixture, two sets of samples (three samples per set) were compacted by a Marshall hammer to achieve air void content of (7 ± 1.0) %. The first set was tested without moisture conditioning. In the second set, the sample was vacuum saturated to obtain a 55 - 80% saturation level, and then the sample was put in the freezer at -18 °C for 16 h. Then, the frozen sample was submerged in the water tank at 60 °C for 24 hr. Finally, the two sets of samples were charged at a 50.8 mm/min rate at a temperature of 25 °C until failure. ITS is calculated by Equation (2) in Kpa.

$$ITS = \frac{2P}{\pi HD} \quad (2)$$

Where P (KN) indicates the peak vertical load, H (mm) is the sample height and D (mm) is the diameter of the asphalt sample.

For each mixture, the tensile strength ratio (TSR) was calculated using Equation (3).

$$TSR\% = 100\left(\frac{ITS_{Wet}}{ITS_{Dry}}\right) \quad (3)$$

Where the ITS_{Wet} refers to the average unconditioned sample ITS, and ITS_{Dry} is the average unconditioned sample ITS.

2.4.2.2 Immersion–compression test

The compressive strength of the base and modified AC mixes was investigated in compliance with ASTM (D-1075) [51]. For this test, the dimensions of the prepared samples are 101.6 mm and 63.5 mm, for height and diameter, respectively. For each percentage of both nanoparticles, six samples were prepared, divided into two groups:

The first group (dry group) is tested after being treated with an air bath at a temperature of 25 °C for 4 hours. The second group (immersed group) is tested after being immersed in a 60 °C water bath for 24 hours and then in another water bath at a temperature of 25 °C for two hours. Axial compression load without lateral support was enforced on the sample at 25±1 °C with a constant rate of 5.08 mm/min, and the peak compressive load was recorded until the sample cracked. The compressive strength value (SC) was computed by using Equation (4) in kg/cm^2, and the index of retained strength (IRS) was calculated according to Equation (5).

$$S_C = \frac{4P}{\pi D^2} \quad (4)$$

$$IRS = \frac{S_{immersed}}{S_{dry}}\ x100 \quad (5)$$

Where:

SC is the compressive strength, kg/cm^2.

P is the peak applied load, kg.

D is the sample diameter, cm.

$S_{immersed}$ and S_{dry} are compressive strength for immersed and dry groups, respectively, kg/cm^2.

2.4.3 Double Punch Test (DPT)

A DPT was performed by Jimenez (1973) at the University of Arizona to study the interlayer debonding of AC mixture [52]. It is repeatable, practical, and appropriate for measuring the field debonding behavior of AC mixtures [53,54]. For each mixture type, three cylindrical samples were prepared with the same dimensions as the Marshall samples. These samples were cured by being placed in the water container for 30 min. at a temperature of 60 °C. This test comprises two 25.4 mm diameter rods (punches) which are precisely centered on both the top and bottom surfaces of the sample. Finally, the sample was tested by charging until collapse with a rate of 25.4 mm/min.

2.4.4 Static creep-recovery test

The static creep test was carried out in conjunction with the UTM Reference Manual and the British Standards Institution [55]. The creep test is the most common test for evaluating the time-dependent properties of an AC mixture by recording the resistance to the formation of the aggregate structure [56]. This test was carried out by enforcing a static load on the AC mixture specimen, and the consequent permanent deformation was gauged over time. The relation recorded in the static creep test is presented in Fig. 5. The test was performed according to the following conditions:

– *Testing temperature*	40 °C,
-*Testing machine*	UTM
– *Applied stress*	100 kPa,
– *Loading time*	3600 sec,

2.4.4.1 Accumulated strain

The accumulated strain $(\varepsilon(t))$ is the ratio between the recorded deformation at any time (Δh) to the original height of the tested sample (h_0). It is deduced from Equation (6)

$$\varepsilon(t) = \frac{\Delta h}{h_0} \quad (6)$$

2.4.4.2 Recovery ratio

The recovery ratio is defined as: the ratio between elastic strain and maximum strain. It can be calculated from Equation (7).

$$R\% = \frac{\varepsilon_{Elast}}{\varepsilon_{Max}} x100 \quad (7)$$

Where:

R= recovery ratio

ε_{Max}= maximum strain (ε_{max}) = total vertical strain at the end of loading (at 3600 sec)

ε_{Elast}= elastic strain = ε_{max} - ε_{perm} = the difference between the maximum and the permanent strain.

2.4.4.3 Stiffness modulus and creep compliance

Stiffness modulus is defined as the division of constant vertical stress on strain at any point in time. Creep compliance is the multiplicative inverse of the stiffness modulus. Stiffness modulus and creep compliance can be calculated using Equation (8) and Equation (9), respectively.

$$S_{mix} = \frac{\sigma}{\varepsilon_s(t)} \quad (8)$$

$$D_{(t)} = \frac{\varepsilon_s(t)}{\sigma} \quad (9)$$

Where:

S_{mix}=stiffness modulus AC mixtures at 40 °C, MPa

σ= applied constant stress, kPa.

$\varepsilon_s(t)$ =strain at any time (t) and a temperature of 40 °C, mm/mm

$D_{(t)}$ =creep compliance as a function in time, 1/MPa

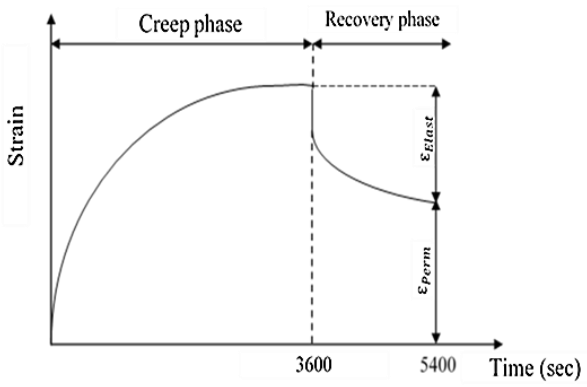

Fig. 5. The typical response of AC mixture under creep-recovery test

III. RESULTS AND DISCUSSION

3.1 Asphalt binder

3.1.1 Effect of nanoparticles on penetration and softening point

Fig. 6 shows the influence of the nanomaterial type and content on the penetration values of the asphalt. For NS modified binder, as the percentage of the modifier increased, a decrease in the penetration occurred from 62 to 39.33 at 2% NS. The same trend occurred with increasing NC% when the penetration value decreased from 62 to 38.67 at 3% NC. In contrast, the penetration value increased with 4% of NC and became 42.33. This may be attributed to the agglomeration of the NC particles at a high percentage, and these results are consistent with Van De Ven et al. [57] and ZareShahabadi et al. [58].

For the softening point test, both NS and NC increased it from 45.4°C to more than 57°C, as shown in Fig. 7. The softening point increased up to 57.3°C and 58.1°C at 3%NS and 3%NC, respectively, then the values slightly decreased afterward. These findings agreed with several studies [21,59,60].

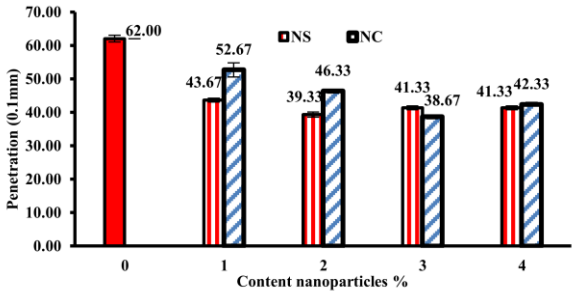

Fig. 6. Penetration versus the percentage of nanoparticles

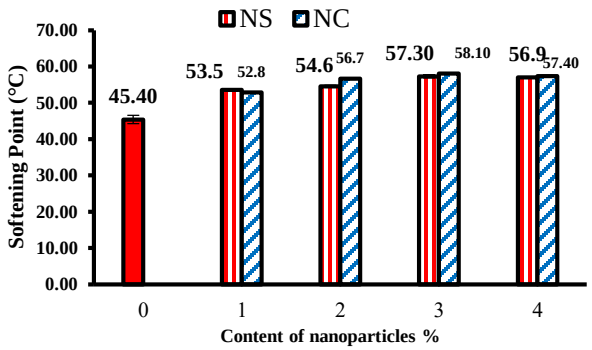

Fig. 7. Softening point versus the percentage of nanoparticles

3.1.2 Thermal sensitivity

To quantify the relative temperature susceptibility the penetration index was used. There is inverse relationship between them [61]. It is obvious from Fig. 8 that PI values increased with increasing the content of both nanoparticles to reach the maximum value at 3% NS and 4% NC. Hence, this indicates that the binders' susceptibility to temperature decreases. This is due to the increase in the surface area of the nanoparticles due to the smaller size of their particles, obtaining a modified asphalt binder that is stiffer and less sensitive to temperature.

3.1.3 Rotational viscosity

Fig. 9 depicts the impact of the nanomaterial contents and temperature on RV viscosity values. At a temperature of 135 °C, increasing the NS to 4% increased the RV viscosity by 101%. On the other hand, NC increased the viscosity at 135 °C by more than 136% at 3%. However, increasing the NC content to 4% decreased the viscosity to 109 % compared to the control asphalt. Ezzat et al. [21] reported performance of NC similar results. The viscosity should not be more than the allowable limit. According to AASH-TO (T-316), the maximum amount for bitumen viscosity is 3000 mpa.s [62].

3.1.4 Storage stability

Storage stability is one of the technical problems facing modified asphalt binders when stored for a long time, especially at high temperatures. The difference in density and solubility factor between asphalt binder and additives causes sedimentation of the additive particles at the bottom of the storage vessel under the influence of gravity. Fig. 10 shows an increase in the difference between top- and bottom- softening point values as nanoparticles percentage increases, indicating a lack of storage stability.

This deficiency is more remarkable in NC compared to NS because the density of Nano-Clay is greater than that of Nano-Silica, and therefore its sedimentation rate is higher. However, the degree of storage stability remains within the recommended limits in ASTM D5892 [41]. Therefore, asphalt modified with Nano-Clay and Nano-Silica with a content of no more than 4% is recommended for use in paving works, even after it has been stored for a long time.

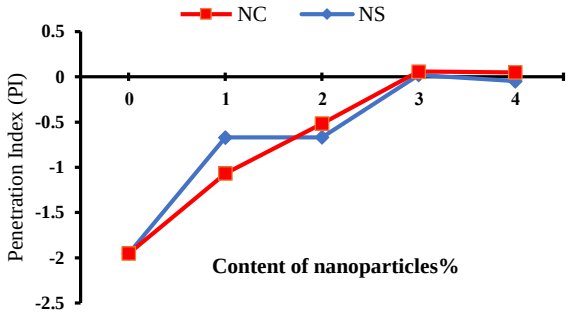

Fig. 8. Penetration index versus the percentage of nanoparticles

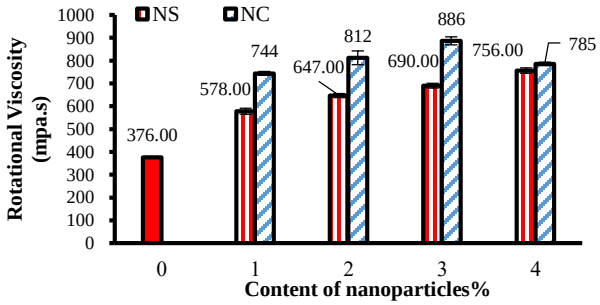

Fig. 9. Rotational viscosity versus the percentage of nanoparticles

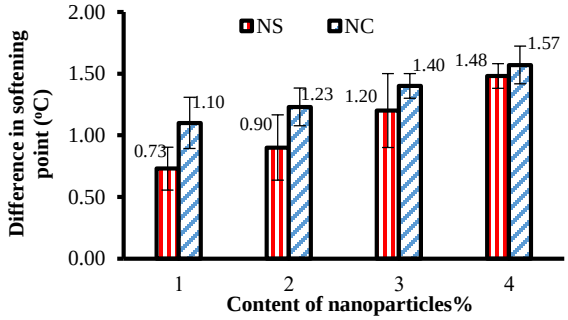

Fig. 10. The difference in softening point between top and bottom versus the percentage of nanoparticles

3.1.5 Structure and morphology of asphalt binder

Fig. 11 shows the electronically scanned images of raw asphalt and nano-modified asphalt. It is noted that the nanomaterials are distributed uniformly within the asphalt binder matrix, which gives an indication of the efficiency of the mixing process using the high shear mixer. However, it is also noted that there is a difference in the structure between raw and modified asphalt binders, which may be explained by the formation of new bonds between asphalt binders and nanomaterials.

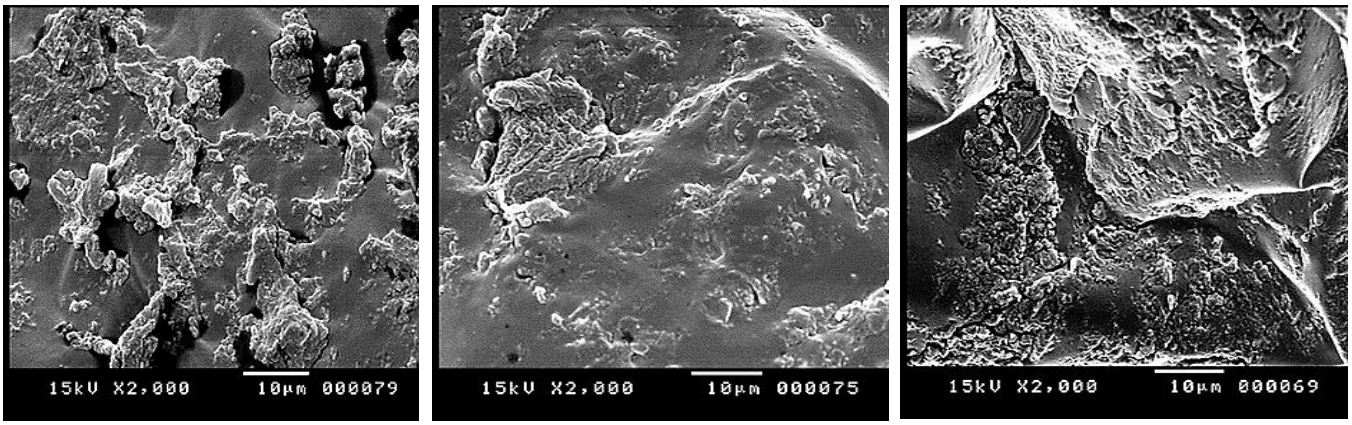

(a) (b) (c)

Fig. 11. SEM images of control and nano-modified binders, (a) control; (b) 3% NC; (c) 3% NS

3.1.6 Fourier Transform Infrared Spectroscopy (FTIR)

The infrared spectra of neat asphalt and nano-modified asphalt are presented in Fig. 12. Table 6 shows the main characteristic absorption peaks in the base and modified binder. In the control asphalt, the adsorption peak at around 3445 cm−1 is ascribed O–H stretch, H-bonded alcohols, phenols. The adsorption peaks at around 2922 cm−1 and 2851 cm−1 are ascribed to C-H aliphatic hydrogen and C-H symmetric stretching (aliphatic), respectively. The peak at around 1615 cm−1 is ascribed to C=C stretch aromatics. Also, C–H bend alkanes and C-H symmetric bending of CH3 from asphalt were generated at 1452 cm−1 and 1376 cm−1., respectively. In the fingerprint region, there was a peak appearing at 721 cm-1 that refers to (CH2) n,n>4. In the NC-modified asphalt, no new peaks are appearing but there was a decrease in intensity compared to the control asphalt. In the NS-modified asphalt, a new functional group was generated at 1086 cm-1, referring to C–O deformation in secondary alcohols and aliphatic esters.

3.2 AC mixture

3.2.1 Marshall test

One of the most important property of AC mixtures is Marshall stability which reflects the resistance of mixture to permanent deformation. The results of stability values of nano modified asphalt mixtures were indicated in Fig. 13. From the previous Figure, the stability was improved with adding the two types of nano-particles. However, the Nano-Clay is more effective than the Nano-Silica on the Marshall stability; the maximum Marshall stability of modified HMA with 3% NC and 4% NS is higher than the stability of the control mix with 33.9% and 13.1%, respectively.

The MQ indicates the resistance of AC mixtures to permanent deformation [71]. Fig. 14 shows the MQ of the modified mixtures with NC and NS, respectively. The MQ increases with increasing Nano-Clay content. This indicates that Nano-Clay improves resistance to permanent deformation. The rigidity of the mixtures is observed to in-crease with increasing the content of Nano-Clay in the mixture up to 4%. The highest rigidity value was sustained at 3% NC with a 39.4% increment than the control mix value.

For NS, MQ values improve with increasing NS dosage to increase by 16.16% at 4% NS. This suggests that AC mixtures modified with NC and NC can be used for paving sites, where AC mixtures with low asphalt concentrations and high stiffness are needed.

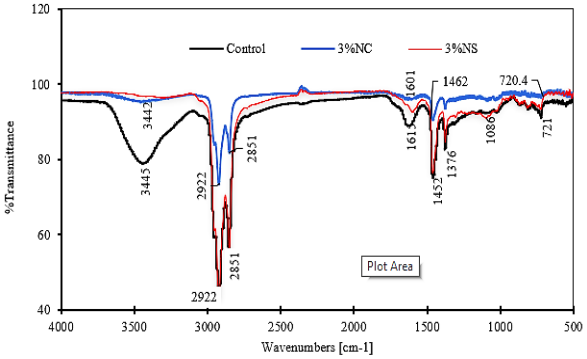

Fig. 12. Infrared spectra for control and nano-modified binders

TABLE VI
FUNCTIONAL GROUPS CORRESPONDING TO WAVE NUMBER [63–70]

Band assignment	Band position (cm^{-1})
(CH_2) n,n >4	720,721
C–O deformation in secondary alcohols and aliphatic esters	1086
C-H symmetric bending of CH3 from asphalt	1376
C–H bend alkanes	1452,1462
C=C stretching (aromatic) from asphalt	1601, 1615
C-H symmetric stretching (aliphatic) from asphalt	2850, 2851
C-H aliphatic hydrogen; CH3 & CH2; asymmetric stretching	2922
O-H stretch, H-bonded alcohols, phenols	3442, 3445

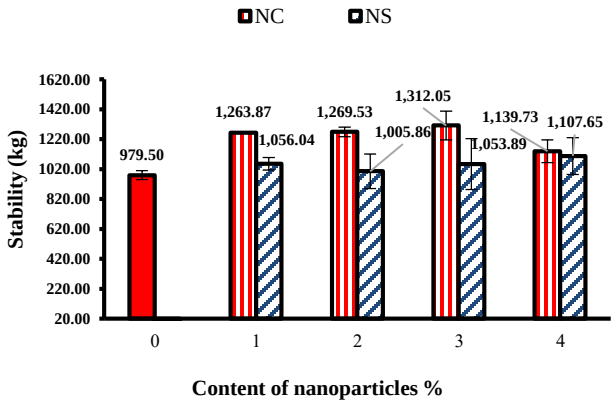

Fig. 13. Marshall stability versus the percentage of nanoparticles in the mixture

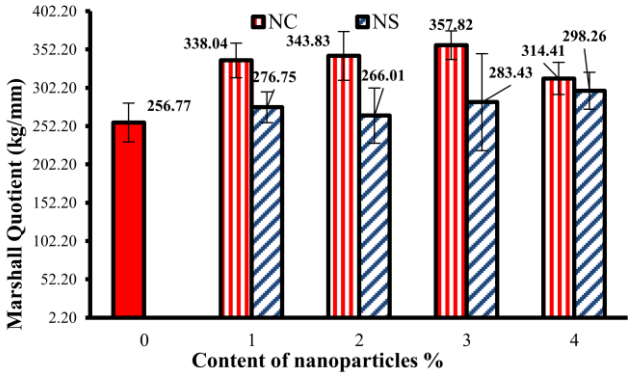

Fig. 14. Marshall quotient (MQ) versus the percentage of nanoparticles in the mixture

3.2.2 Moisture susceptibility

One of the experimental tests that reflect thermal and fatigue cracking resistance of AC mixtures is the ITS. Figs. 15 and 16. show the ITS values for conditioned and unconditioned control and nano-modified mixtures. In dry and wet conditions of AC mixtures, the ITS values increased with adding either Nano-Clay or Nano-Silica. Moreover, the ITS of the conditioned mixtures is lower than that of the dry ones. This explains clearly the effect of moisture on AC mixtures which expressed as moisture damage. When this difference was decreased, the resistance of moisture damage was improved. It noticed also, the difference decreases with increasing contents of either Nano-Clay or Nano-Silica. Nevertheless, Nano-Clay is more effective than Nano-Silica in improving this resistance to moisture damage. The resistance of AC mixtures to moisture damage can be measured by the TSR of the AC mixtures.

TSR increases with increasing Nano-Clay and Nano-Silica content. Nano-Clay is more effective than Nano-Silica in improving resistance to moisture damage. According to ECP, the tensile strength ratio (TSR) between the IDT values for conditioned and non-conditioned mixtures should be higher than 75% [32]. While all modified mixtures satisfy the requirement, the mixture containing 4% NS has a lower TSR than the minimum requirement.

Immersion–Compression test is one of the tests that assess moisture susceptibility by calculating the index of retained strength (IRS). The outcomes of the test are summarized in Figs. 17 and 18. The results reveal an improvement in dry and wet strength value by increasing the nano-content in the mixtures. In the case of the modified mixtures with Nano-Clay at 4% NC, there was an increase in the strength by 67% and 94% in the dry and wet conditions, respectively. In contrast, there was an increase in strength by 43% and 69% for NS-modified mixtures in the dry and wet conditions, respectively, at 4% NS.

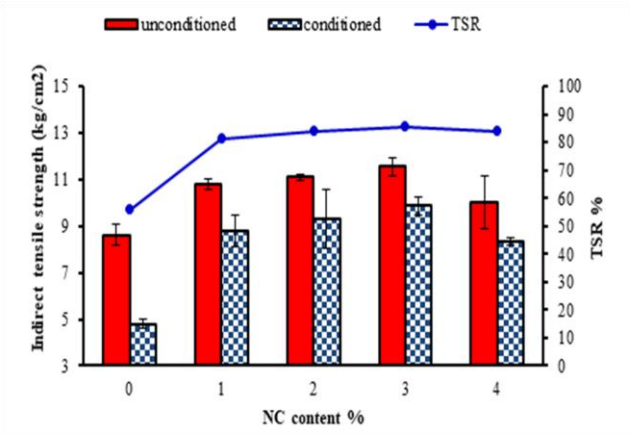

Fig. 15. Indirect tensile strength results of control and NC-modified mixtures

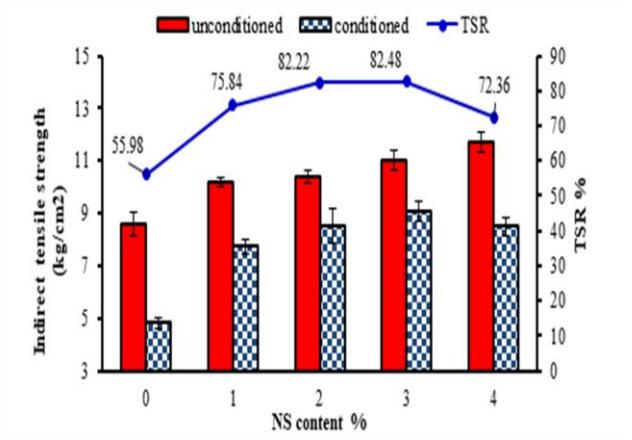

Fig. 16. Indirect tensile strength results of control and NS-modified mixtures

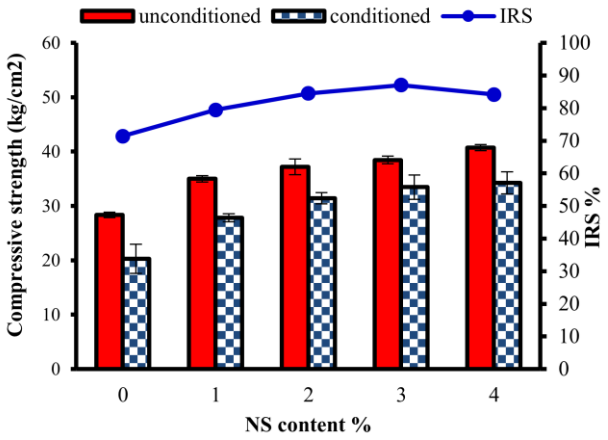

Fig. 17. Compressive strength results of control and NS-modified mixtures

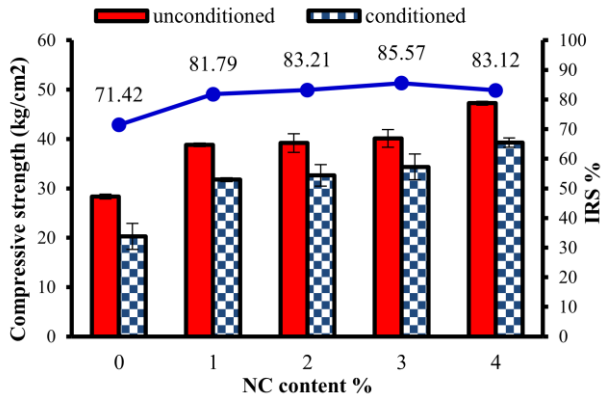

Fig. 18. Compressive strength results of control and NC-modified mixtures

3.2.3 Debonding resistance

The double punch test indicates the debonding behavior between binder and aggregate. The effect of the addition of Nano-Clay and Nano-Silica on the double punch values is shown in Fig. 19. The double punch values for all modified binders were increased with increasing NC or NS content up to 4% compared with the control binder, but NS has a more pronounced effect in improving the bonding properties of a mixture that provides the required elasticity and plasticity characteristics and enhances the viscosity of the binder.

3.2.4 Rutting resistance

The accumulated axial strain was measured during 3600 sec. of continuous loading, followed by the recovery time of 1800 sec. The accumulated strain was drawn at a selected temperature of 40 °C for control and modified samples. As shown in Fig. 20, the increase in strain leads to a higher potential for rutting, and decreasing the stiffness. Accordingly, AC mixtures will not sustain the static load. The NC and NS specimens showed a clear reduction in axial strain, as seen below. It is also clear that adding any of the modifiers (NC or NS) has decreased strain values, which is a good indication of their significant role in increasing the mixture's resistance to rutting.

Fig. 21 presents the results of permanent strain and the recovery ratio of AC mixtures. These results are significantly depending on the type and content of nanomaterial. From this test, a lower strain is sustainable with better a rut-resistant mixture. As shown, the lowest permanent strain was achieved with adding the nanomaterials when compared to the control mixture. This refers to a better resistance to the permanent deformation as expected under traffic loads. The recovery and, therefore rutting resistance could be enhanced if a higher percentage of nanoparticles is utilized to the mixture. Generally, incorporation of nanoparticles lead to decline both of permanent and recovery strain.

The outputs for creep stiffness are summarized in Fig. 22. The results revealed an improvement in the HMA ability to resist deflection caused by an applied load due to increased stiffness modulus and increased nanoparticles dosage. NC-modified mixtures had the best performance as they had the highest stiffness modulus, while NS had a lower stiffness modulus value than NC-modified mixtures. The stiffness value was improved compared to the control mixture by 62% and 57% at 4% NC and 2% NS, respectively.

This indicates that the performance of NC was better than that of NS in improving the dry and wet strength value. When calculating IRS, it was found that the highest values occurred at 3% of nanoparticles, but NS was more effective with a value greater than 87% at 3% NS, compared to 85% at 3% NC.

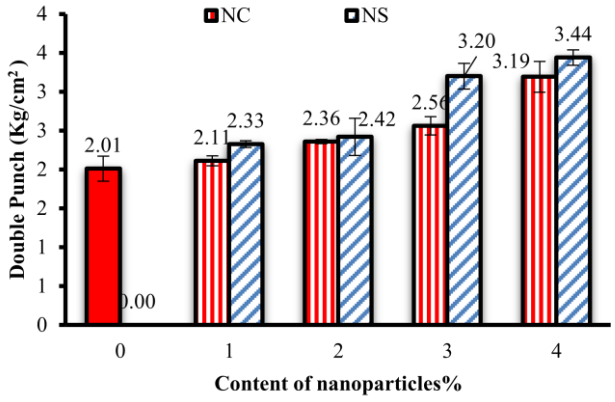

Fig. 19. Double punch versus the percentage of nanoparticles in the mixture

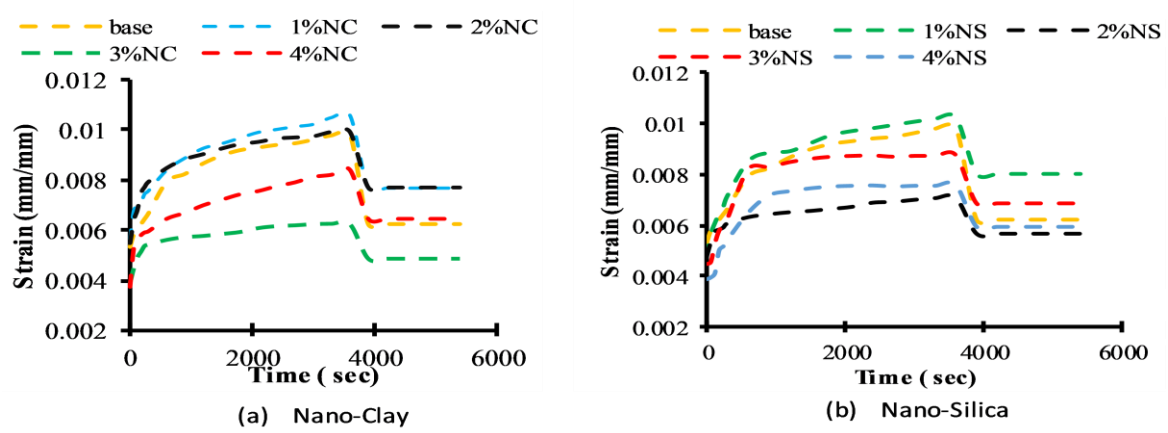

Fig. 20. Accumulated axial strain for nano-modified mixtures at 40 °C

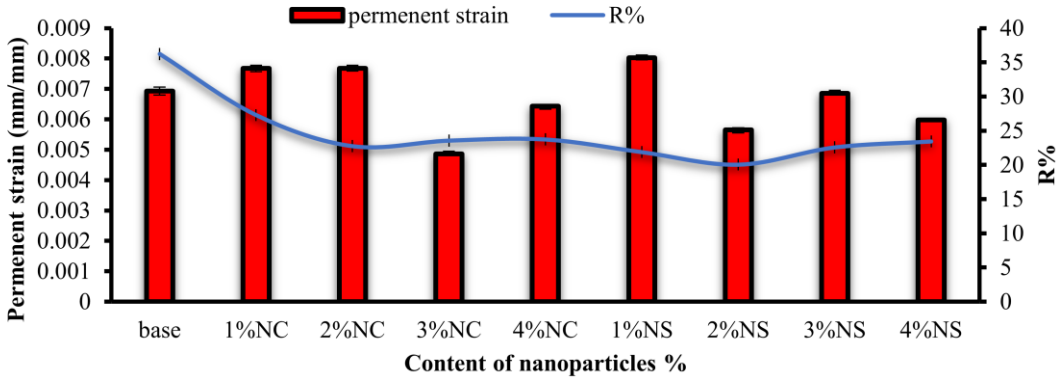

Fig. 21. Permanent strain recovery ratio for control and nano-modified mixtures

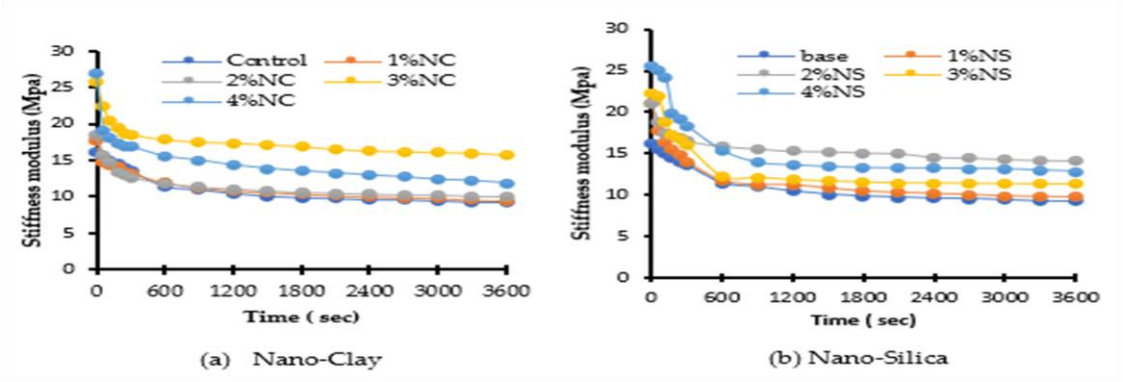

Fig. 22. Stiffness modulus for control and nano-modified mixtures

IV. CONCLUSIONS

In this study, effects of incorporating two different types of nanomaterials (NS and NC) on the performance of asphalt binders and mixes were investigated. The following conclusions can be drawn based on the obtained results:

- The binder's physical testing results show that adding nanoparticles can increase softening point and rotational viscosity and decrease penetration depth of the binder.
- Nanomaterials reduce the asphalt binder's thermal sensitivity.
- Increasing nanoparticles contents, the binder's storage stability decreases but remains within the permissible limits.
- For both nano materials (NC and NS), nanoparticles disperse well within the asphalt binder matrix without clustering based on SEM photos.
- FTIR test revealed that the mixing process of nanomaterials with the base asphalt was not a chemical process as no new functional groups appeared in nano-modified asphalt binder compared to control asphalt.
- Nanoparticles had a significant impact on increasing the stiffness and moisture damage susceptibility while reducing the debonding tendency of AC mixtures.
- Comparison between the effect of NC and NS on the performance of the AC mixtures (stability, debonding, moisture damage, and rutting): Both types of nanoparticles improved the performance of the mixture, but the performance of NC was better in most tests.
- Based upon the laboratory tests carried out in this research, the addition of 3% and 4% of Nano-Clay and Nano-Silica, respectively, could be concluded as an optimal percentage for improving control mixtures in different tests.

V. ACKNOWLEDGEMENTS

The authors are appreciative the co-operation of all members of the Highway and Airport Engineering Laboratory at Sohag University and Assiut University in accomplishing the current study.

AUTHORS CONTRIBUTION

Talaat Abdel-Wahed, conceptualization, formal analysis, methodology, and writing review and editing.

Ashraf Abdel-Raheem, writing original draft, formal analysis.

Ghada S. Moussa, review and editing.

FUNDING STATEMENT:

No financial support was received

DECLARATION OF CONFLICTING INTERESTS STATEMENT:

The author declared that there are no potential conflicts of interest with respect to the research authorship or publication of this article.

REFERENCES

[1] H. Taherkhani, S. Afroozi, Investigating the Performance Characteristics of Asphaltic Concrete Containing Nano-Silica, Civ. Eng. Infrastructures J. (Journal Fac. Eng. 50 (2017) 75–93. https://doi.org/10.7508/ceij.2017.01.005.

[2] G. Moussa, I. Sallam, H. Younis, Performance Investigation Of Hot-And Warm-Asphalt Mixtures Modified With Superplast. JES. Journal of Engineering Sciences, (2021) 49(5), pp.679-703. https://doi.org/ 10.21608/JESAUN.2021.82128.1060.

[3] H.K. Shanbara, A. Dulaimi, T. Al-Mansoori, S. Al-Busaltan, M. Herez, M. Sadique, T. Abdel-Wahed, The future of eco-friendly cold mix asphalt, Renew. Sustain. Energy Rev. 149 (2021) 111318.

[4] G.S. Moussa, A. Abdel-Raheem, T. Abdel-Wahed, Effect of Nanoclay Particles on the Performance of High-Density Polyethylene-Modified Asphalt Concrete Mixture, Polym.. 13 (2021). https://doi.org/10.3390/polym13030434.

[5] G. Moussa, A. Abdel-Raheem, T. Abdel-Wahed, INVESTIGATING THE MOISTURE SUSCEPTIBILITY OF ASPHALT MIXTURES MODIFIED WITH HIGH-DENSITY POLYETHYLENE, JES. J. Eng. Sci. 48 (2020) 765–782.

[6] A.H. Abed, A.M. Oudah, Rheological properties of modified asphalt binder with nanosilica and SBS, IOP Conf. Ser. Mater. Sci. Eng. 433 (2018) 12031. https://doi.org/10.1088/1757-899X/433/1/012031.

[7] R. Li, F. Xiao, S. Amirkhanian, Z. You, J. Huang, Developments of nano materials and technologies on asphalt materials – A review, Constr. Build. Mater. 143 (2017) 633–648. https://doi.org/10.1016/j.conbuildmat.2017.03.158.

[8] F.M. Nejad, H. Nazari, K. Naderi, F. Karimiyan Khosroshahi, M. Hatefi Oskuei, Thermal and rheological properties of nanoparticle modified asphalt binder at low and intermediate temperature range, Pet. Sci. Technol. 35 (2017) 641–646.

[9] H. Yao, Z. You, L. Li, C.H. Lee, D. Wingard, Y.K. Yap, X. Shi, S.W. Goh, Rheological properties and chemical bonding of asphalt modified with nanosilica, J. Mater. Civ. Eng. 25 (2013) 1619–1630. https://doi.org/10.1061/(asce)mt.1943-5533.0000690.

[10] C. Fang, R. Yu, S. Liu, Y. Li, Nanomaterials applied in asphalt modification: A review, J. Mater. Sci. Technol. 29 (2013) 589–594. https://doi.org/10.1016/j.jmst.2013.04.008.

[11] J. Tanzadeh, F. Vahedi, T.K. Pezhouhan, R. Tanzadeh, Laboratory study on the effect of nano Tio2 on rutting performance of asphalt pavements, Adv. Mater. Res. 622 (2013) 990–994. https://doi.org/10.4028/www.scientific.net/AMR.622-623.990.

[12] H. Taherkhani, S. Afroozi, The properties of nanosilica-modified asphalt cement, Pet. Sci. Technol. 34 (2016) 1381–1386. https://doi.org/10.1080/10916466.2016.1205604.

[13] T.A. Abdel-Wahed, N.K. Rashwan, Application of Cement Dust and OPC as Mineral Filler in the binder Hot Mix Asphalt, Eng. Infrastruct. 15 (2016).

[14] T.A. Abdel-Wahed, N.K. Rashwan, A.E. Maurice, The physical properties of bitumen modified with ilmenite and bentonite nanoparticles, HBRC J. 16 (2020) 335–350.

[15] H. Taherkhani, M. Tajdini, Comparing the effects of nano-silica and hydrated lime on the properties of asphalt concrete, Constr. Build. Mater. 218 (2019) 308–315. https://doi.org/10.1016/j.conbuildmat.2019.05.116.

[16] K.A. Masri, H. Awang, R.P. Jaya, M.I. Ali, N.I. Ramli, A.K. Arshad, Moisture susceptibility of porous asphalt mixture with Nano silica modified asphalt binder, in: IOP Conf. Ser. Earth Environ. Sci., 2019: p. 12028. https://doi.org/10.1088/1755-1315/244/1/012028.

[17] H.H. Zghair, H.H. Joni, M.S. Hassan, Impact of Mi xing process on the physical and Rheological Characteristics of Asphalt Binder Modified with Nano- Silica Powder, IOP Conf. Ser. Mater. Sci. Eng. 579 (2019). https://doi.org/10.1088/1757-899X/579/1/012046.

[18] H.H. Zghair, H. Jony, M. Hassan, Rheological Characteristics of Nano Silica Modified Asphalt Binder Material, Proc. 5th Int. Eng. Conf. IEC 2019. (2019) 79–84. https://doi.org/10.1109/IEC47844.2019.8950636.

[19] F. Zafari, M. Rahi, N. Moshtagh, H. Nazockdast, The Improvement of Bitumen Properties by Adding NanoSilica, 3 (2014) 62–69.

[20] A. Kavussi, P. Barghabani, The Influence of Nano Materials on Moisture Resistance of Asphalt Mixes, 3 (2014) 36–40.

[21] H. Ezzat, S. El-Badawy, A. Gabr, E.S.I. Zaki, T. Breakah, Evaluation of Asphalt Binders Modified with Nanoclay and Nanosilica, in: Procedia Eng., 2016. https://doi.org/10.1016/j.proeng.2016.06.119.

[22] H. Taherkhani, S. Afroozi, Investigating the creep properties of asphaltic concrete containing nano-silica, Sadhana - Acad. Proc. Eng. Sci. 43

(2018) 1–9. https://doi.org/10.1007/s12046-018-0792-3.
[23] M. Sadeghnejad, G. Shafabakhsh, Use of Nano SiO2 and Nano TiO2 to improve the mechanical behaviour of stone mastic asphalt mixtures, Constr. Build. Mater. 157 (2017) 965–974. https://doi.org/10.1016/J.CONBUILDMAT.2017.09.163.
[24] G. Shafabakhsh, S.M. Mirabdolazimi, M. Sadeghnejad, Evaluation the effect of nano-TiO2 on the rutting and fatigue behavior of asphalt mixtures, Constr. Build. Mater. 54 (2014) 566–571. https://doi.org/10.1016/J.CONBUILDMAT.2013.12.064.
[25] M. Sadeghnejad, G. Shafabakhsh, Experimental Study on the Physical and Rheological Properties of Bitumen Modified with Different Nano Materials (Nano SiO2 & Nano TiO2), Int. J. Nanosci. Nanotechnol. 13 (2017) 253–263.
[26] J. Tanzadeh, R. Tanzadeh, H. Nazari, N. Kamvar, Fatigue Evaluation of Hot Mix Asphalt (HMA) Mixtures Modified by Optimum Percent of TiO2 Nanoparticles, Adv. Eng. Forum. 24 (2017) 55–62. https://doi.org/10.4028/www.scientific.net/aef.24.55.
[27] M. Saltan, S. Terzi, S. Karahancer, Examination of hot mix asphalt and binder performance modified with nano silica, Constr. Build. Mater. 156 (2017) 976–984. https://doi.org/10.1016/j.conbuildmat.2017.09.069.
[28] M.G. Al-Taher, H.D. Hassanin, M.F. Elgendy, A.M. Sawan, Improving the Performance of Asphalt Mixtures Using Nano Silica, World Appl. Sci. J. 35 (2017) 2614–2621.
[29] M. Zakaria, M. El, M. Zahw, E.S. Mosa, Study the Effect of Nano-Kaolinite on the Properties of Bitumen and Asphalt Mixtures, (2017).
[30] G.H. Hamedi, F.M. Nejad, K. Oveisi, Estimating the moisture damage of asphalt mixture modified with nano zinc oxide, Mater. Struct. Constr. 49 (2016) 1165–1174. https://doi.org/10.1617/s11527-015-0566-x.
[31] M. Saltan, S. Terzi, S. Karahancer, Performance analysis of nano modified bitumen and hot mix asphalt, Constr. Build. Mater. 173 (2018) 228–237. https://doi.org/10.1016/j.conbuildmat.2018.04.014.
[32] Egyptian code of practice for urban and rural road's part 4: road material and its tests, Housing and Building National Research Center, Egypt, 2018.
[33] ASTM (2006) Terminology for nanotechnology. E2456-06. American Society for Testing and Materials. www.liu.se. Accessed 15 February 2010, (n.d.). http://www.liu.se.
[34] D. ASTM, D1559-89, Stand. Test Method Resist. to Plast. Flow Bitum. Mix. Using Marshall Appar. Annu. B. ASTM Stand. USA. (2003).
[35] D. ASTM, Standard test method for penetration of bituminous materials, USA, ASTM Int. (2013).
[36] D. ASTM, Standard test method for softening point of bitumen (ring-and-ball apparatus), American Association of State and Highway Transportation Officials, Washington, DC, 2014.
[37] A. D2171/D2171M, Standard test method for viscosity of asphalts by vacuum capillary viscometer, Am. Soc. Test. Mater. Int. (2010).
[38] J. Read, D. Whiteoak, R.N. Hunter, The shell bitumen handbook, Thomas Telford, 2003.
[39] L.Y. Ming, C.P. Feng, E.A.A. Siddig, Effect of phenolic resin on the performance of the styrene-butadiene rubber modified asphalt, Constr. Build. Mater. 181 (2018) 465–473. https://doi.org/10.1016/j.conbuildmat.2018.06.076.
[40] B. Amini, M.J. Rajabbolookat, A. Abdi, R. Salehfard, Investigating the influence of using nano-composites on storage stability of modified bitumen and moisture damage of HMA, Pet. Sci. Technol. 35 (2017) 800–805. https://doi.org/10.1080/10916466.2017.1292292.
[41] A. D5892, Standard Specification for Type IV Polymer-Modified Asphalt Cement for Use in Pavement Construction, (2000).
[42] R. Li, J. Pei, C. Sun, Effect of nano-ZnO with modified surface on properties of bitumen, Constr. Build. Mater. 98 (2015) 656–661. https://doi.org/10.1016/j.conbuildmat.2015.08.141.
[43] N.I.M. Yusoff, A.A.S. Breem, H.N.M.M. Alattug, A. Hamim, J. Ahmad, The effects of moisture susceptibility and ageing conditions on nano-silica/polymer-modified asphalt mixtures, Constr. Build. Mater. 72 (2014) 139–147. https://doi.org/10.1016/j.conbuildmat.2014.09.014.
[44] H.V. Vo, D.-W. Park, Application of conductive materials to asphalt pavement, Adv. Mater. Sci. Eng. 2017 (2017).
[45] M. Mubaraki, The Effect of Modified Asphalt Binders by Fourier Transform Infrared Spectroscopy, X-Ray Diffraction, and Scanning Electron Microscopy, 6 (2019) 5–14.
[46] W. Saowapark, C. Jubsilp, S. Rimdusit, Natural rubber latex-modified asphalts for pavement application: effects of phosphoric acid and sulphur addition, Road Mater. Pavement Des. 0 (2017) 1–14. https://doi.org/10.1080/14680629.2017.1378117.
[47] A. Mansourian, A.R. Goahri, F.K. Khosrowshahi, Performance evaluation of asphalt binder modified with EVA/HDPE/nanoclay based on linear and non-linear viscoelastic behaviors, Constr. Build. Mater. 208 (2019) 554–563. https://doi.org/10.1016/j.conbuildmat.2019.03.065.
[48] Y. Sheng, B. Zhang, Y. Yan, H. Chen, R. Xiong, J. Geng, Effects of phosphorus slag powder and polyester fiber on performance characteristics of asphalt binders and resultant mixtures, Constr. Build. Mater. 141 (2017) 289–295. https://doi.org/10.1016/j.conbuildmat.2017.02.141.
[49] H.A.A.A. Gibreil, C.P. Feng, Effects of high-density polyethylene and crumb rubber powder as modifiers on properties of hot mix asphalt, Constr. Build. Mater. 142 (2017) 101–108. https://doi.org/10.1016/j.conbuildmat.2017.03.062.
[50] AASHTO T283-14, Standard Method of Test for Resistance of Compacted Asphalt Mixtures to Moisture-Induced Damage, Am. Assoc. State Highw. Transp. Off. Washington, DC. 14 (2014).
[51] Standard Test Method for Effect of Water on Compressive Strength of Compacted Bituminous Mixtures. ASTM D1075–11, ASTM International, West Conshohocken, PA, 2011.
[52] R.A. Jimenez, Testing for debonding of asphalt from aggregates, (1973).
[53] R.A. Jimenez, Field Control Test for Debonding of Asphalt Concrete, Transp. Res. Rec. 1228 (1989) 1–8.
[54] B.M. Kiggundu, F.L. Roberts, Stripping in HMA mixtures: State-of-the-art and critical review of test methods, (1988).
[55] B. Standard, Method for assessment of resistance to permanent deformation of bitumen aggregate mixtures Subject to Unconfined Uniaxial Loading, Draft Dev. DD. 185 (1996).
[56] P.J. Van de Loo, Creep Test: A Key Tool in Asphalt Mix Design and In the Prediction of Pavement Rutting, in: Assoc. Asph. Paving Technol. Proc, 1978.
[57] M.F. Van De Ven, A.A. Molenaar, J. Besamusca, J. Noordergraaf, Nanotechnology for binders of asphalt mixtures, in: Proc. 4TH EURASPHALT EUROBITUME Congr. HELD MAY 2008, COPENHAGEN, DENMARK, 2008.
[58] A. Zare-Shahabadi, A. Shokuhfar, S. Ebrahimi-Nejad, Preparation and rheological characterization of asphalt binders reinforced with layered silicate nanoparticles, Constr. Build. Mater. 24 (2010) 1239–1244.
[59] M. El-Shafie, I.M. Ibrahim, A.M.M.A. El Rahman, The addition effects of macro and nano clay on the performance of asphalt binder, Egypt. J. Pet. 21 (2012) 149–154.
[60] M.F.C. Van de Ven, A.A.A. Molenaar, J. Besamusca, Nanoclay for binder modification of asphalt mixtures, in: Proc. 7th Int. RILEM Symp. Adv. Test. and. Charact. Bitum. Mater. Rhodes, Greece, 2009: pp. 133–142.
[61] A.K. Arshad, M.S. Samsudin, J. Ahmad, K.A. Masri, Microstructure of nanosilica modified binder by atomic force microscopy, J. Teknol. 78 (2016).
[62] Standard method of test for viscosity determination of asphalt binder using rotational viscometer, American Association of State and Highway Transportation Officials, Washington, DC, 2013.
[63] A.D.S. Araujo, V.D.F.C.D.F.C. Lins, M.D. Pasa, M. De Fa, M. de F.A. de S. Araujo, V.D.F.C.D.F.C. Lins, V.M.D. Pasa, C.G. Fonseca, A.D.S. Araujo, V.D.F.C.D.F.C. Lins, M.D. Pasa, M. De Fa, Infrared Spectroscopy Study of Photodegradation of Polymer Modified Asphalt Binder, J. Appl. Polym. Sci. 125 (2012) 3275–3281. https://doi.org/10.1002/app.
[64] H.L. Zhang, H.C. Wang, J.Y. Yu, Effect of aging on morphology of organo-montmorillonite modified bitumen by atomic force microscopy, J. Microsc. 242 (2011) 37–45.
[65] H. Yao, Q. Dai, Z. You, Fourier Transform Infrared Spectroscopy characterization of aging-related properties of original and nano-modified asphalt binders, Constr. Build. Mater. 101 (2015) 1078–1087. https://doi.org/10.1016/j.conbuildmat.2015.10.085.
[66] H. Yao, Z. You, L. Li, S.W. Goh, C.H. Lee, Y.K. Yap, X. Shi, Rheological properties and chemical analysis of nanoclay and carbon microfiber modified asphalt with Fourier transform infrared spectroscopy, Constr. Build. Mater. 38 (2013) 327–337.
[67] C. Fang, R. Yu, Y. Li, M.M. Zhang, J. Hu, M.M. Zhang, Preparation and characterization of an asphalt-modifying agent with waste packaging polyethylene and organic montmorillonite, Polym. Test. 32 (2013) 953–960. https://doi.org/10.1016/j.polymertesting.2013.04.006.
[68] G. Malarvizhi, R. Sabermathi, C. Kamaraj, Laboratory study on nano clay modified asphalt pavement, Int. J. Appl. Eng. Res. 10 (2015) 20175–20190.
[69] A.D.S. Araujo, V.D.F.C. Lins, M.D. Pasa, M. De Fa, Infrared Spectroscopy Study of Photodegradation of Polymer Modified Asphalt Binder, (2012). https://doi.org/10.1002/app.

[70] K. Bukka, J.D. Miller, A.G. Oblad, Fractionation and characterization of Utah tar-sand bitumens: Influence of chemical composition on bitumen viscosity, Energy & Fuels. 5 (1991) 333–340.
[71] S.E. Zoorob, L.B. Suparma, Laboratory design and investigation of the properties of continuously graded Asphaltic concrete containing recycled plastics aggregate replacement (Plastiphalt), Cem. Concr. Compos. 22 (2000) 233–242.

Title Arabic:

التحقق من أداء الخليط الأسفلتي المعدل بجزيئات النانو

Arabic Abstract:

حاليًا، تم استخدام المواد النانوية على نطاق واسع لتحسين خصائص الإسفلت نظرًا لخصائصها الفريدة. يهدف هذا البحث إلى تقييم أداء الاسفلت المعدل بنوعين مختلفين من المواد النانوية، وهما النانو سيليكا والنانو كلاي. تمت إضافة كل منهما إلى بيتومين 70/60 بتركيزات تتراوح من 1٪ إلى 4٪ من وزن الأسفلت باستخدام خلاط عالي القص بسرعة 4000 دورة في الدقيقة ودرجة حرارة خلط 145 درجة مئوية لمدة 60 دقيقة. تم إجراء عدد من الاختبارات الأساسية على البيتومين المعدل، مثل اختبار الغرز، واختبار التطرية، واللزوجة الدوارة، واختبار ثبات التخزين، بالإضافة إلى فحص المجهر الإلكتروني واختبار FTIR .أجريت كل هذه الاختبارات للتأكد من جودة عملية الخلط وللتحقق من التركيب الداخلي للبيتومين المعدل. علاوة على ذلك، تم إجراء دراسة معملية إضافية لتوصيف خصائص أداء الخلطات الإسفلتية بناءً على ثبات مارشال، وقوة الشد غير المباشرة، وقابلية الرطوبة، واختبار الثقب المزدوج، والزحف. بناءً على النتائج التجريبية، تم تحقيق أفضل أداء عند إضافة من 3-4٪ من الجسيمات النانوية مع مادة الأسفلت الخام. بشكل عام، فإن إضافة جزيئات النانو سيليكا والنانو كلاي كان لها تأثير إيجابي على الخصائص المختلفة للأسفلت والخليط الأسفلتي من حيث الثبات، والتعرية، وتلف الرطوبة، والتشقق. ومع ذلك، كان النانو كلاي أكثر فعالية مقارنة بـ نانو سيليكا.

Talaat Abdel-Wahed is an Associate Professor in the department of Civil Engineering, Faculty of Engineering, Sohag University, Egypt. He received his Ph.D. in Civil Engineering from Menoufia University, Egypt, in 2011. His fields of interest include consistency of highway geometric design, traffic performance analysis, pavement maintenance and rehabilitation, improvement of mechanical properties of hot and cold asphalt mix, asphalt pavement technology such as hot asphalt mixture design.

Ashraf Abdel-Raheem is an assistant lecturer in the Civil Engineering Department, Faculty of Engineering, Sohag University. He completed his undergraduate studies at Sohag University (2017) and started working as an assistant lecturer in December 2020. His fields of interest include performance enhancement of Hot Mix Asphalt (HMA) using polymers and nanomaterials and finite element analyses of pavements.

Ghada S. Moussa is a Professor of Highway and Traffic Engineering in the Civil Engineering Department, Faculty of Engineering, Assiut University, and the Director of the Highways Laboratory, Assiut University. She obtained her M.S. in Structural Engineering and Ph.D. in Transportation Engineering both from the University of Central Florida, the USA.
Her major research interests include pavement material characterization and analysis, traffic data modeling, accident analysis, highway safety, machine learning, and deep learning. She has published many studies in well-reputable journals.